Observation of Bulk and Edge Magnetoplasmons in a Two-Dimensional Electron Fluid

D. B. Mast
Department of Physics, University of Cincinnati, Cincinnati, Ohio 45221

and

A. J. Dahm
Department of Physics, Case Western Reserve University, Cleveland, Ohio 44106

and

A. L. Fetter
Institute of Theoretical Physics, Department of Physics, Stanford University, Stanford, California 94305
(Received 8 January 1985)

Two-dimensional magnetoplasmons are studied in a classical gas of electrons bound to a liquid-helium surface. A new and unpredicted resonant mode has been observed. The density and magnetic field dependences of this new mode differ strikingly from normal magnetoplasmons. These new resonant modes are interpreted as edge magnetoplasmons of the two-dimensional charge sheet.

PACS numbers: 73.20.Cw, 52.35.−g, 71.45.Gm

Two-dimensional (2D) electron systems have been of wide experimental and theoretical interest for several years. Theoretically, the reduced degrees of freedom allow detailed and often exact calculations. Experimentally, new, unexpected phenomena have been observed. While 2D systems display analogs of characteristics of 3D systems, the lower dimensionality often modifies their properties dramatically. Plasmons of a classical 2D electron gas are a case in point.

We report an experimental and theoretical investigation of plasmon resonances in a classical 2D Coulomb gas of electrons, trapped in surface states above a liquid-helium surface, when a magnetic field is applied perpendicular to the charge layer. We observe two sets of resonant absorption spectra. One set is the normal plasmon-cyclotron coupled modes. An additional set of resonant spectra has mode frequencies that decrease dramatically with increasing magnetic field. We identify these latter resonances as edge plasmons of the 2D charge sheet—the 2D analog of surface plasmons in 3D systems. To our knowledge these are the first edge modes observed in a 2D system.

The plasmons of a 2D electron sheet were first observed by Grimes and Adams.[1] They confirmed the 2D plasmon dispersion relation in zero field[2]:

$$\omega_p^2 = 4\pi ne^2 k/m\,[\epsilon \coth(kh) + \coth(ks)].$$

Here e and m are the electronic charge and mass, n is the electron areal density, k is the wave vector, ϵ is the dielectric constant of liquid helium, and h and s are, respectively, the separation of the electrons from grounded planes below and above the sample. If a magnetic field is applied perpendicular to an unbounded electron sheet, the plasmon frequency is predicted to shift to[3] $\omega = (\omega_p^2 + \omega_c^2)^{1/2}$, where $\omega_c = eB/mc$.

We study plasmons in an applied magnetic field with an experimental cell and procedures similar to those of Grimes and Adams.[1] Our 2D electron sample is confined between the plates of a rectangular cross-section, parallel-plate capacitor semi-immersed in liquid helium.[4] The sample density is fixed by the potential difference between the top and bottom plates. Each capacitor plate has dimensions $(W = 1.78$ cm$) \times (L = 2.5$ cm) and is divided into three equal-area electrodes. Our procedure for observing these resonant modes involves exciting standing-wave resonances in the electron sheet, and recording the power absorbed by the electrons as a function of the excitation frequency. These standing waves are generated by application of a small ac voltage to the top center electrode, which produces a small ac change in the electron areal density under this electrode. The boundary conditions select wave vectors, $k_x = m\pi/W$ and $k_y = n\pi/L$ $m \neq 3l$, where m, n, and l are even integers.

Typical traces of the rf absorption are shown in Fig. 1. The upper trace shows the normal plasmon resonances in zero magnetic field. The arrows are the calculated zero-field plasmon frequencies labeled with mode integers m and n. The lower trace is typical of the new resonances that we have observed. These modes have been observed in the temperature range from $T \simeq 0.90$ K, where vapor-atom scattering broadens the resonances, down to the melting temperature of the 2D Wigner cyrstal. We have not fully investigated whether these modes can propagate in the solid phase. For densities $\geq 2\times 10^8$ cm^{-2} the amplitudes of the new peaks decrease rapidly as the solid phase begins to form. This decrease may result from additional damping in the solid phase.

A plot of experimental standing-wave resonance fre-

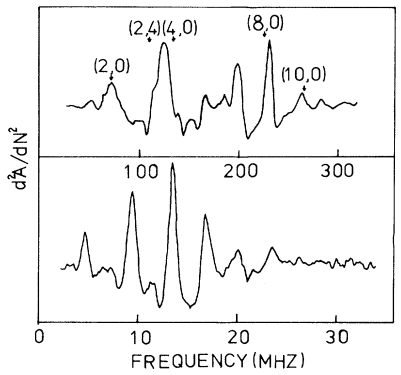

FIG. 1. Experimental traces of the second derivative with respect to density of the rf absorption plotted vs frequency. The upper trace shows the normal plasmon standing-wave resonances in zero magnetic field; $n = 1 \times 10^8$ cm^{-2}. The lower trace shows the resonant peaks of the new absorption mode in a magnetic field of 765 G; $n = 3 \times 10^8$ cm^{-2}.

quencies as a function of applied field is shown in Fig. 2. The various curves are associated with different wave vectors. Data were taken at different densities in different magnetic field regimes as indicated in the figure caption. The zero of the magnetic field is uncertain to ± 10 G as a result of trapped flux near our sample.

We associate the resonances which shift to higher frequencies with increasing magnetic field with the normal 2D plasmons. In Fig. 3 we plot the squares of the angular frequencies of the normal plasmon modes versus ω_c^2 for a different sample. The curves are labeled with the mode integers (m,n). The lowest curve represents an overlap of the (2,4) and (4,0) resonances and the identification of another curve is uncertain. For $\omega_c > 1.5 \times 10^9$ sec^{-1} the line shapes were distorted. This distortion and the deviation from the theoretical curves in Fig. 2 may be due to an overlap with other resonances as the lines broadened with increasing field.

The dominant feature in Fig. 2 is a new branch of the magnetoplasmon dispersion relation which is not present in an infinite 2D electron sheet. For a fixed wave vector, the standing wave frequencies vary as B^{-1} for large magnetic fields and, in the limit of zero field, extrapolate to a value below the corresponding plasma resonances of the upper branch. The amplitudes of the new-mode absorption spectra are smaller than the upper-branch peaks by a factor of approximately 5. These amplitudes decrease linearly with increasing temperature. In fields of order 700 G the quality factor of these modes is $\simeq 3$ and the linewidths are an order of magnitude smaller than the linewidths of the normal plasmons in zero field. In large magnetic fields the frequencies of these modes are linear in density.[5] The measurements reported here were taken

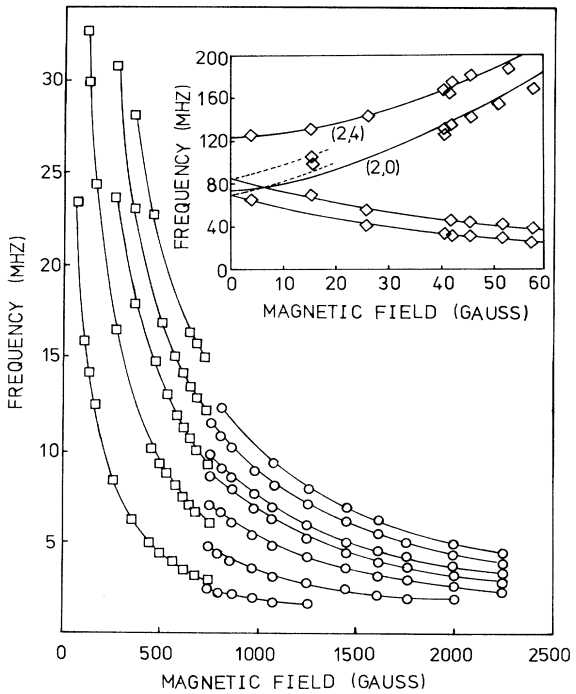

FIG. 2. Plot of standing-wave frequencies vs applied magnetic field. The inset shows two branches of the spectrum at small fields. The symbols are as follows: squares, $n = 2.8 \times 10^8$ cm^{-2}; circles, $n = 2 \times 10^8$ cm^{-2}; lozenges, $n = 1.2 \times 10^8$ cm^{-2}. The curves are theoretical fits to the data. There are no adjustable parameters for the normal magnetoplasmon modes labeled with mode integers (m,n).

at the saturated density, $n_s = E_\perp / 2\pi e$. The holding field, $E_\perp$, is not expected to have any additional influence on the frequency.

Our theoretical picture of these phenomena relies on the hydrodynamic model of a charged compressible

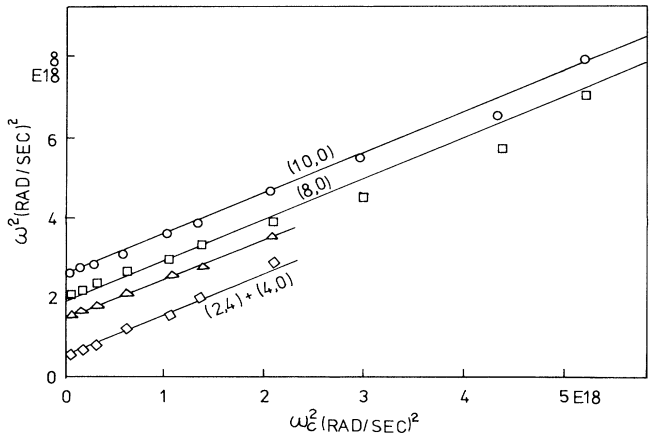

FIG. 3. Square of the upper-branch angular frequency vs ω_c^2 for four wave vectors; $n = 1.1 \times 10^8$ cm^{-2}. The lines are drawn with a slope of unity.

fluid placed in a uniform neutralizing background.[6] This model includes dispersion, which arises from the compressibility, and screening, but it omits retardation. In three dimensions, it allows an exact solution for bulk magnetoplasmons with general wave number. It also describes surface magnetoplasmons bound to a 3D half-space; if the field is parallel to the surface and the surface wave propagates perpendicular to the field, the long-wavelength dispersion relation[7] is given by the roots of the equation $2\omega^2 \pm 2\omega\omega_c - \Omega_p^2 = 0$, where $\Omega_p - (4\pi e^2 n/m)^{1/2}$ is the bulk 3D plasma frequency and the plus/minus sign reflects the two different directions of propagation relative to the field. Since the product of the roots is independent of ω_c, whereas the sum is proportional to ω_c, one root behaves like ω_c^{-1} for $\omega_c/\Omega_p >> 1$.

Although the preceding analysis suggests 2D "edge" magnetoplasmons as the explanation of the lower modes seen in Fig. 2, the greatly reduced screening in 2D requires a separate and more intricate analysis. We again use the hydrodynamic model without retardation. With a magnetic field $B\hat{z}$ perpendicular to an unbounded layer, the dynamical equations for the electron fluid (conservation of matter and momentum) are essentially those for the 3D case. In contrast, Poisson's equation $\nabla^2\Phi = 4\pi e n'\delta(z)$ must be solved for the potential Φ arising from the density perturbation n' in the layer. A straightforward analysis for a plane wave reproduces the long-wavelength result noted previously; in particular, the frequency of all bulk 2D magnetoplasmons increases with increasing applied field.

We next consider a half-sheet for $x < 0$, with a wave $\propto e^{iky}$ propagating along the boundary. The right-hand side of Poisson's equation now vanishes for $x > 0$; a Fourier transform in x then yields an integral relation $\Phi(x,z=0) = -4\pi e\int_{-\infty}^{0} dx' L(x-x')n'(x')$ between the potential Φ in the plane of the layer and the density perturbation. Here, $L(x) = (2\pi)^{-1}K_0(k|x|)$ is the inverse transform of $\frac{1}{2}(k^2+k'^2)^{-1/2}$. In principle, when combined with the dynamical equations for the fluid, this problem can be solved with Wiener-Hopf techniques[8]; unfortunately, the details become cumbersome, and we instead replace L by an approximate kernel $2^{-3/2}\exp(-2^{1/2}k|x|)$, with equal area and second moment.[8] The resulting approximate model can now be solved *exactly*. Imposing the conditions that the velocity v_x vanish at $x=0$, and that Φ and its gradient be continuous there, we eventually obtain the equation $3\omega^2 \pm 2^{3/2}\omega\omega_c - 2\omega_p^2 = 0$ for the dispersion relation of long-wavelength edge magnetoplasmons bound to the half-layer. Here ω_p is the 2D plasma frequency for wave number k in zero field, and the plus/minus sign again arises from the two field directions relative to y. Apart from the altered numerical constants and the appearance of the appropriate 2D plasma frequency, this equation is very similar to that for 3D surface magnetoplasmons.[7] In particular, one root,

$$|\omega_-| = (2^{1/2}/3)[(3\omega_p^2+\omega_c^2)^{1/2} - \omega_c], \quad (1)$$

has all the features seen in Fig. 2, and we therefore tentatively identify the lower mode as an edge magnetoplasmon of the 2D charge sheet.

In Figs. 4 and 5, we compare our data with the predictions for ω_- given by Eq. (1). The two lower curves shown in the inset in Fig. 2 are plotted in Fig. 4 as $(|\omega_-| + 2^{1/2}\omega_c/3)^2$ vs ω_c^2. The least-squares–fitted slopes are 0.227 ± 0.006, where the errors include an uncertainty in the zero of field. The solid line represents the theoretical value of $\frac{2}{9}$.

We analyze the intermediate-field data by writing

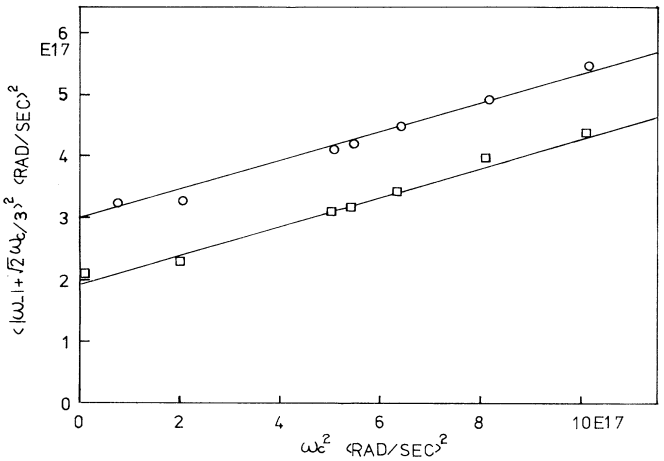

FIG. 4. The quantity $(|\omega_-| + 2^{1/2}\omega_c/3)^2$ vs ω_c^2 for $n = 1.2\times10^8$ cm^{-2} and small magnetic fields. The two curves represent different wave vectors.

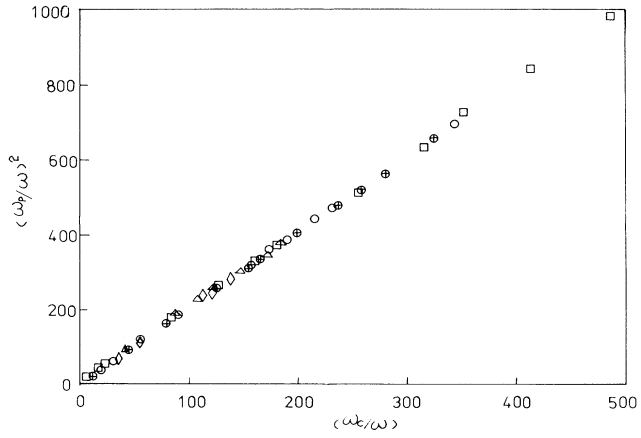

FIG. 5. The intermediate-field data for ω_- plotted as $(\omega_p/\omega)^2$ vs ω_c/ω. The density is 2.8×10^8 cm^{-2}. Different symbols represent different wave vectors.

the dispersion relation as $(\omega_p/\omega_-)^2 - b(\omega_c/|\omega_-|) - a = 0$ and allow a and b to be adjustable parameters. Figure 5 is a graph of $(\omega_p/\omega_-)^2$ vs ω_c/ω_- for the intermediate-field resonant modes shown in Fig. 2. The values of ω_p associated with these modes is uncertain and was used as an adjustable parameter. Both the intermediate- and high-field data (Fig. 2) are in excellent qualitative agreement with the theory, which it must be remembered involves one basic approximation. The intercept a is uncertain because of the sensitivity to the determination of zero field (± 10 G). If we assign the mode numbers (2,0) to the lowest-frequency edge modes, we obtain $a - \simeq 1.1$ and $b \simeq 1$ from Fig. 4 and $b \simeq 2$ from Fig. 5; an obvious discrepancy for the parameter b. However, these numerical values are very uncertain since it is difficult to assign wave vectors, and thus to determine values of ω_p, for the edge modes. The approximate theoretical values are $a = 1.5$ and $b = 2^{1/2}$.

The theory of edge magnetoplasmons gives excellent qualitative agreement with the experimental data. The theory predicts that the penetration depth from the edge of the sample for this excitation is $\simeq k^{-1}$. For the lowest mode excited on opposite sides of the sample, a fraction $2/k_x L = W/\pi L = 0.22$ of the electrons are involved in the excitation. This is consistent with a signal amplitude which is approximately 20% of the amplitude of the normal-plasmon signals. The narrow linewidth of these resonances relative to the normal plasmons raises an interesting theoretical question which we have not yet investigated.

It is unlikely that we have observed the upper, ω_+, edge magnetoplasmon branch which is drawn as dashed curves in the inset of Fig. 2. At small fields a number of edge modes at differing wave vectors have absorption peaks that overlap other normal-mode peaks, and it is difficult to resolve the absorption spectra. It is possible that the other edge branch is not discernible for the same reason.

In conclusion, we have investigated the dispersion of 2D plasmons in an applied magnetic field. For the normal plasmon resonances, we find reasonable agreement between theory and experiment. In addition, we have observed a new resonant mode in the 2D electron gas. We solved for the collective modes of a 2D plasma in a half-plane placed in a magnetic field and obtained the dispersion relation for a new set of propagating modes, which we call 2D edge magnetoplasmons. These calculations are in qualitative agreement with the experimental data.

After this work was submitted, we received a preprint from D. C. Glattli, E. Y. Andrei, G. Deville, J. Poitrenaud, and F. I. B. Williams which reports an investigation of magnetoplasmons in a similar system.

We wish to thank H. W. Jiang and M. A. Stan for their help with the data reduction. Stimulating conversations with J. D. Maynard, J. A. Northby, and R. G. Petschek are gratefully acknowledged. This work was supported, in part, by the National Science Foundation under Grants No DMR-82-13581 and No. DMR-81-18386.

[1]C. C. Grimes and G. Adams, Phys. Rev. Lett. **36**, 145 (1976).

[2]This equation is an adaptation of Eq. (4) of A. V. Chaplik, Zh. Eksp. Teor. Fiz. **62**, 746 (1972) [Sov. Phys. JETP **35**, 395 (1972)]. See also C. C. Grimes and G. Adams, Surf. Sci. **58**, 292 (1976).

[3]N. J. M. Horing and M. Yildiz, Phys. Lett. **44A**, 386 (1973).

[4]R. Mehrotra, C. J. Guo, Y. Z. Ruan, D. B. Mast, and A. J. Dahm, Phys. Rev. B **29**, 5239 (1984).

[5]A plot of the density dependence of the boundary magnetoplasmon standing-wave frequencies at fixed magnetic field has been given by D. Mast and A. J. Dahm, Physica (Utrecht) **126B**, 457 (1985).

[6]G. Barton [Rep. Prog. Phys. **42**, 65 (1979)] treats the hydrodynamic model in detail.

[7]3D surface magnetoplasmons have been considered by K. N. Stepanov, Zh. Tekh. Fiz. **35**, 1349 (1965) [Sov. Phys. Tech. Phys. **10**, 1048 (1966)]; and K. W. Chiu and J. J. Quinn, Phys. Rev. B **5**, 4707 (1972). The associated magnetic field dependence is implicit in Fig. 3 of J. J. Brion, R. F. Wallace, A. Hartstein, and E. Burstein, Surf. Sci. **34**, 73 (1973); the corresponding experiments are reported in A. Hartstein and E. Burstein, Solid State Commun. **14**, 1223 (1974).

[8]G. F. Carrier, M. Krook, and C. E. Pearson, *Functions of a Complex Variable* (McGraw-Hill, New York, 1966), Secs. 8-1, 8-3, and 8-4.